

The Dutch PV Portal 2.0

An Online Photovoltaic Performance Modeling Environment for the Netherlands

Schepel, Veikko ; Tozzi, Arianna ; Klement, Marianne ; Ziar, Hesan; Isabella, Olindo; Zeman, Miro

DOI

[10.1016/j.renene.2019.11.033](https://doi.org/10.1016/j.renene.2019.11.033)

Publication date

2020

Document Version

Final published version

Published in

Renewable Energy

Citation (APA)

Schepel, V., Tozzi, A., Klement, M., Ziar, H., Isabella, O., & Zeman, M. (2020). The Dutch PV Portal 2.0: An Online Photovoltaic Performance Modeling Environment for the Netherlands. *Renewable Energy*, 154, 175-186. <https://doi.org/10.1016/j.renene.2019.11.033>

Important note

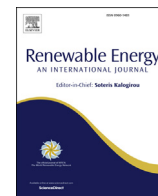
To cite this publication, please use the final published version (if applicable). Please check the document version above.

Copyright

Other than for strictly personal use, it is not permitted to download, forward or distribute the text or part of it, without the consent of the author(s) and/or copyright holder(s), unless the work is under an open content license such as Creative Commons.

Takedown policy

Please contact us and provide details if you believe this document breaches copyrights. We will remove access to the work immediately and investigate your claim.



The Dutch PV portal 2.0: An online photovoltaic performance modeling environment for the Netherlands

Veikko Schepel, Arianna Tozzi, Marianne Klement, Hesam Ziar*, Olindo Isabella, Miro Zeman

Photovoltaic Materials and Devices Group (PVMD), Delft University of Technology, Mekelweg 4, 2628, CD, Delft, the Netherlands

ARTICLE INFO

Article history:

Received 19 June 2019

Received in revised form

11 October 2019

Accepted 8 November 2019

Available online 9 November 2019

Keywords:

Photovoltaic system

Online performance modeling

Meteorological data

Real-time solar energy conversion

National solar electricity production

Netherlands

ABSTRACT

This paper describes the core model that lies behind an online modeling environment for photovoltaic (PV) energy generation in the Netherlands, called the Dutch PV Portal 2.0 (PVP 2.0). PVP 2.0 realizes three functionalities: (i) a real-time system efficiency breakdown figure, (ii) an estimate of national solar electricity production, and (iii) an economic analysis for small-scale to large scale PV systems. The unique and novel aspects of this website are the dynamically updated climate database, the rainfall-dependent soiling loss calculation, and the orientation-dependent inverter sizing factor. This paper also justifies the PVP 2.0 capabilities in large scale studies. First, the PVP 2.0 modeling approach was validated by yield comparison with 26 real PV systems distributed over the Netherlands. The validation resulted in -11% to $+5.5\%$ deviation from measured data. Then, a back-end sensitivity study found that a rain-free summer in the Netherlands results in an AC energy loss of 3.4% in that period, while a change in wind speed or ambient temperature could lead to losses around 2–4.5 GWh/year (0.58%–1.16%) on province scale. The core of the approach presented in this paper can be used to develop similar websites for other countries of interest with adapted add-ons depending on the target climate condition. Such study tools could eventually provide more quantitative insights about the impact of climate change (by applying probable scenarios) on the renewable energy production of the World.

© 2019 Published by Elsevier Ltd.

1. Introduction

In the past decade, the global installed capacity of PV systems has grown exponentially, reaching 0.5 TW_p in 2018 [1]. With the rising importance of PV, publicly accessible and reliable information is necessary for contributing to public understanding and support of this energy alternative. A major pathway through which this knowledge transfer can be enabled is the internet. Numerous solar electricity websites have been developed that aim to educate visitors on PV. Some websites focus on interactive elements that allow users to design a PV system and calculate its expected energy production. Notable examples are PV Education [2], the PV Performance Modeling Collaborative of Sandia National Laboratories [3], Sunny Design [4], and PVGIS [5]. Next to these websites which have an international scope, there are also more location-specific websites focusing on photovoltaic potential within a certain

country. Notable examples are ZonAtlas (the Netherlands) [6], Google's Project Sunroof (the U.S.A.) [7], and the Slovenian PV Portal (Slovenia) [8].

A useful role can be played by universities and research institutes that actively develop new knowledge of PV. Information communicated by these institutes is scientifically accurate and incorporates innovative elements or new developments in the field of PV. At the Photovoltaic Materials and Devices (PVMD) research group of Delft University of Technology, a solar electricity website titled the Dutch PV Portal was launched in 2014 (as communicated in Ref. [9]). A unique feature of this website is that it uses real-time meteorological data measured at Dutch weather stations to calculate the real-time performance of designed PV systems. Although the Dutch PV Portal is not a commercial product, such as PVsyst [10], Meteonorm [11], Sungevity [12], or Solar Monkey [13], it does apply complex, up-to-date and accurate physical models for PV energy calculation while also providing information on photovoltaics for laymen for the geographic region of the Netherlands. In March 2018, a second version of the Dutch PV Portal (PVP 2.0), was launched. The PVP 2.0 was created by developing five main

* Corresponding author.

E-mail address: h.ziar@tudelft.nl (H. Ziar).

elements (Fig. 1).

This paper reports on the methodology through which each of the elements was developed in a general manner, to allow the method to be adapted to other countries besides the Netherlands. The paper also highlights several unique features of the PVP 2.0 compared to other solar electricity modeling environments. The ultimate aim is to establish a tool that, besides the conventional features of PV prediction websites, can also perform sensitivity analysis to evaluate the effect of probable climate change scenarios on solar energy production. The rest of the paper is organized as follows. First, the creation of the meteorological database is described, followed by an explanation of the components of the PV system performance model and the way the meteorological data are used in the model. Then, three sections are dedicated to the description of the efficiency breakdown, the national solar electricity production, and the economic analysis elements of the website. Finally, the last section describes a yield comparison and sensitivity study as a first validation of the PVP 2.0 performance model. The last section highlights conclusions and remarks.

2. Meteorological database

2.1. Database description

Determining the performance of a PV system at a given moment in time requires answers to two questions: (1) what are the meteorological conditions at the PV system at that moment and (2) how will the PV system perform under these meteorological conditions? The creation of a meteorological database is, therefore, an essential element for a PV system modeling environment.

The PVP 2.0 uses two types of meteorological datasets: an annual dataset with an hourly time resolution, and a daily (real-time) dataset with a 10-min time resolution. The annual dataset is used to calculate the annual PV system performance, whereas the real-time dataset is used to calculate the daily and real-time system performances. Both datasets store the same 11 meteorological variables as shown in Table 1, of which 7 are measured by the Dutch meteorological institute (Koninklijk Nederlands Meteorologisch Instituut (KNMI)).

In Table 1, DirHI is the projection of the direct normal irradiance (DNI) on the horizontal plane. The parameters in Table 1 can be separated into two groups. Global, diffuse, and direct horizontal irradiance are used in conjunction with Sun azimuth and altitude to calculate the initial plane-of-array irradiance (G_{PoA}) falling on a PV module. The other six parameters are used (together with the G_{PoA}) to calculate the deviation of the real module efficiency from the efficiency at standard test conditions (STC). This aspect will be elaborated in Section 3.

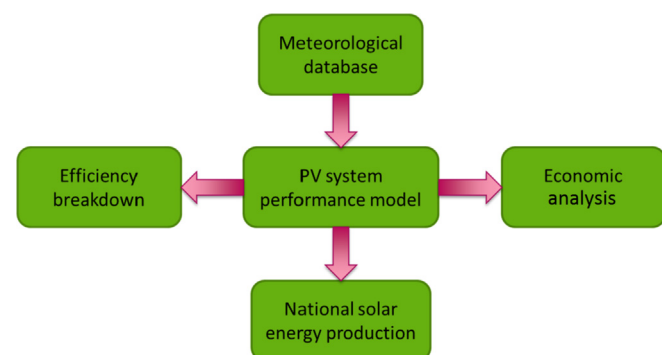


Fig. 1. Main elements of the PVP 2.0. The arrows denote the flow of information between elements.

Table 1

Parameters stored in the PVP 2.0 meteorological database.

Meteorological parameters	Source
Global horizontal irradiance (GHI) [W/m ²]	KNMI weather station
Ground temperature [°C]	KNMI weather station
Ambient temperature [°C]	KNMI weather station
Cloud cover [okta]	KNMI weather station
Wind speed [m/s]	KNMI weather station
Pressure [Pa]	KNMI weather station
Rainfall [mm/hr]	KNMI weather station
Diffuse horizontal irradiance (DHI) [W/m ²]	Calculated via Reindl model [14]
Direct horizontal irradiance (DirHI) [W/m ²]	Calculated via Reindl model [14]
Sun azimuth [°]	Calculated via equations described in Ref. [15]
Sun altitude [°]	Calculated via equations described in Ref. [15]

2.2. Database structure

The measurement parameters are collected from 46 weather stations of the KNMI. Real-time data are retrieved every 10 min from the KNMI server. The annual datasets were constructed through publicly available historic measurements of the KNMI.

Commonly, a typical meteorological year (TMY) is used for calculating PV system performance, which selects the weather data of a specific year that has the lowest standard deviation from the long-term (10–15 years of the weather at a certain location) [16]. All major meteorological sources for PV system modeling provide either a TMY or the opportunity to select the weather of one specific year, as listed in an overview by Ref. [17]. In the PVP 2.0, a different and novel type of annual dataset was constructed for PV system performance modeling: a climate dataset. Instead of using weather data of one year, a long-term moving average for every hour timeslot is calculated using the data of every timeslot measurement since 1991. An annual dataset consisting of these 8784 (24×366) hourly timeslot averages is equivalent to a dataset representing the climate (i.e. the 27-year weather average) for that location [18].

The reason a climate average dataset is used is primarily to be able to incorporate the real-time weather measurements in long-term storage in the climate dataset. This is done by creating a weighted average of real-time measurement and the long-term climate average of the corresponding hourly timeslot. Consequently, the annual dataset becomes dynamic automatically, being updated every hour with new measurements. This is a dataset feature which is not present in other modeling environments. A major advantage of this approach is that the value of every meteorological parameter at every timeslot represents the most common weather condition for that timeslot over the past 27 years. An additional advantage is that the storage of a single climate year significantly lowers the required database storage capacity compared to a database with 27 consecutive years of weather measurements. A disadvantage of the approach is that the climate dataset has a lower hour-to-hour parameter variability than that of a TMY. This is due to the smoothing effect of the inter-annual averaging. Fig. 2 shows the connection between the real-time and annual datasets.

Website users are able to select any location in the Netherlands with an interactive map. Through the nearest neighbor selection, the weather station closest to the user location is chosen. At most, any location in the Netherlands is 35 km away from any of the 46 stations. According to Ref. [19], weather data can reasonably be used within a radius of 50 km around a weather station. When developing a PV portal for countries with a higher distance between weather stations or with a terrain that varies significantly in

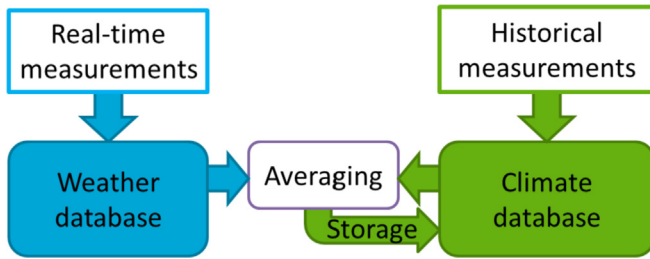


Fig. 2. Overview of the real-time (weather) and historical (climate) database setup, as well as the interconnection between the two databases. The blue color coding indicates the involvement of weather data and the green color coding indicates climate data.

altitude, interpolation methods such as inverse distance weighting (IDW) or kriging can be applied to derive the weather conditions at an arbitrary location from measurements of multiple surrounding weather stations [20].

The real-time and annual datasets of all 46 weather stations are publicly accessible for download and can be used in personal modeling efforts of the PVP 2.0 website visitors.

The data stored in the PVP 2.0 is used to calculate the performance of PV systems according to the model explained in Section 3. In order to construct a similar meteorological database for another country, it is important that the country has a network of reliable weather stations and that the meteorological institute is able and willing to share the real-time and historical data. Satellite weather measurements may be an alternative data source for constructing the datasets.

3. Performance model

3.1. Model components

On the PVP 2.0 website, an option exists for users to design their own PV system by defining characteristics such as installation location, PV array tilt and azimuth, and module technology. The meteorological data and specific characteristics of PV systems, together with scientific insights on how they influence the performance of PV modules and balance of system (BoS) components, are used to calculate the power output of the PV system at every timeslot. The exact power output (P_{PV}) is achieved through two main steps: calculation of the incident plane-of-array irradiance (G_{PoA} , in W/m^2) and calculation of the PV system efficiency (η_{PV}). P_{PV} is then calculated as:

$$P_{PV} = G_{PoA} \cdot \eta_{PV} \cdot A_{PV}, \quad (1)$$

where A_{PV} is the cumulative module surface area (m^2). The PVP 2.0 model distinguishes between two types of PV systems in the calculation of G_{PoA} and η_{PV} : (1) free-standing (field) PV systems and (2) building-added (rooftop) PV systems (BAPV). For field PV systems, the option exists to select a Dutch province and to specify which percentage of the province should be covered with PV panels, in order to show the potential energy generation that could be achieved in that province. Datasets of the calculation results can be downloaded from the website by users for further data analysis. The implementation of East-West, as well as bi-facial design configurations, are planned in a future release of the website.

3.2. Plane-of-array irradiance

G_{PoA} is the intensity of sunlight received on the geometrical plane in which the PV modules are oriented, defined by the module tilt and azimuth. The irradiation impinging on PV module (obtained

using meteorological data), before reaching PV cells, will face losses. In the PVP 2.0 model, G_{PoA} is calculated as:

$$G_{PoA} = G_{PoA-incident} \cdot \eta_{shading} \cdot \eta_{soiling} \cdot \eta_{reflectance}, \quad (2)$$

where $G_{PoA-incident}$ is the incident irradiance excluding light capture losses, and $\eta_{shading}$, $\eta_{soiling}$, and $\eta_{reflectance}$ are the efficiencies that incorporate the various light capture losses before the photons enter the solar panel. $G_{PoA-incident}$ is the sum of the beam (direct), diffuse and albedo components of sunlight:

$$G_{PoA-incident} = G_{beam} + G_{PoA-diffuse} + G_{albedo} \quad (3)$$

$G_{PoA-incident}$ is calculated using the tilted surface model of Reindl et al. [21]. This model uses the data on GHI, module orientation, and Sun position to calculate each component. A surface albedo value of 0.15 was hardcoded for urban (rooftop) environments and a value of 0.24 for non-urban (field) environments [22]. Once $G_{PoA-incident}$ is calculated, it is then de-rated with a chain of efficiencies representing light capture losses.

3.2.1. Shading

Shading is the blocking of sunlight by a surrounding object that would otherwise fall unhindered on the PV module [23]. For a realistic estimate of the amount of shading occurring in each timeslot, sophisticated simulations use a map of the horizon surrounding the PV module together with information on the Sun position. This horizon can either be constructed by using a 360° on-site photograph or by using detailed height profile data for the location (e.g. LiDAR data¹). For the PVP 2.0, both options were not available. The first option requires an on-site visit of the installation location, and the second requires intensive computation, both of which are not feasible for a rapid online performance calculation for any location in the Netherlands.

As an alternative approach, a dataset of 5398 PV systems was used, provided by the company Solar Monkey [13]. This dataset contained an estimate of the annual shading loss for rooftop PV systems using LiDAR data. Therefore, the detailed height profile approach is indirectly used in the PVP 2.0. The average annual shading loss of the systems in the dataset is 6.88%. For rooftop PV systems, this translates to a $\eta_{shading}$ of 93.12%. In the PVP 2.0, no shading loss is considered for free-standing field PV systems as they are assumed to be horizon-free.

In other countries, shading losses for rooftop systems may differ from the losses in the Netherlands. If a dataset like the one of Solar Monkey is available for a country, a shading loss value for that country can be established in the same manner. In the absence of such a dataset, the shading loss of 6.88% used in the PVP 2.0 could be used as an approximation.

The PVP 2.0 shading approach is a simplified solution for multiple reasons. Firstly, it assumes the same loss for any rooftop system regardless of the actual surroundings. Secondly, the same shading loss is applied to every timeslot, although in reality shading loss will depend on the Sun position relative to the surrounding objects. An interactive method for configuring shading losses will be implemented in a future release of the website to override the default value of $\eta_{shading}$.

For field PV systems, it is necessary to mention how the Ground Cover Ratio (GCR, the percentage of total field surface area effectively covered by solar panels) is calculated, as this relates to the amount of inter-row shading that is experienced by the field PV

¹ LiDAR stands for Light Detection And Ranging, a method to measure surface morphology with laser beams.

system. The distance between panel rows is set such that no inter-row shading occurs between 10 a.m. and 3 p.m. on 21 December (the shortest day of the year in the Northern Hemisphere) [15]. Consequently, it is assumed that the effect of inter-row shading in field systems on annual energy production is negligible. Optimally oriented PV systems (South-facing, 37° tilt) have a GCR of 26% in the PVP 2.0. In the next version of the website, it will be possible for users to select a higher GCR, and inter-row shading losses will then be considered in the model.

3.2.2. Soiling

Soiling is the accumulation of dust on a panel surface that absorbs and reflects parts of the incident sunlight. The efficiency loss associated with soiling depends on multiple factors: the amount of dust present in the air and the degree to which rainfall can provide intermittent cleaning of a soiled module [24]. The innovative model applied in the PVP 2.0 is referred to as a rain-free period (RFP) model, developed by Nepal [25]. The dynamic, day-to-day soiling loss calculation of this model is another original feature of the PVP 2.0. In this model, dust accumulates on the panel in periods in which no significant rainfall occurs (the RFP, expressed in days). The effect of dust accumulation on efficiency loss is expressed in a soiling factor (SF), which has a unit of %/day. By multiplying the current RFP and the SF, the current $\eta_{soiling}$ is calculated:

$$\eta_{soiling} = 1 - (RFP \cdot SF) \quad (4)$$

Inferring the current SF from measured environmental parameters is complex and requires several simplifying assumptions that introduce significant uncertainty in the SF calculation [25]. To avoid calculating the SF for every timeslot, in the PVP 2.0 model a fixed SF is used, based on experimental measurements of the soiling loss of multiple PV systems in Delft by Nepal [25]. An SF of 0.083%/day was reported. Pending future experimental research for other locations in the country, this SF was applied to all locations in the Netherlands. The value of SF will be different in countries with other climates and air quality. For example, Kimber et al. [26] found a performance loss of 0.1–0.3%/day for PV systems in California. Country- or region-specific experiments are needed to find an accurate value for SF.

The same series of experiments reported in Ref. [25] found that 2 mm of rainfall was sufficient to clean the panels of all dust. The PVP 2.0 records the rainfall measurements of weather stations and uses these to keep track of the current RFP for all stations. If on a day no rainfall occurs, the RFP of the next day is equivalent to the RFP of the day before, incremented by one day, and the soiling loss of the next day will thus be 0.083% higher. In case that more than 0 mm but less than 2 mm of rainfall occurs, the RFP of the next day is kept equal to that of the previous day, assuming that no further dust deposition takes place on a day with light rainfall. If 2 mm of rainfall or more occurs on a day, the RFP during the next day will be reset to zero, and consequently there will be no soiling loss on that day as the panel is completely clean. The described algorithm is summarized in Fig. 3.

With the PVP 2.0 climate datasets, an annual average RFP for the Netherlands of 3.1 days was calculated. After the implementation of the soiling loss model, the annual soiling loss for the Netherlands was found to be only ~0.3%/year. To adapt this shading model for another region/country, RFP and SF for that region/country must be known. RFP can be obtained using the meteorological database of the target region/country (in desert areas RFP could be very long during dry years) and SF can be obtained by field experiments. In this way, the soiling model implemented in PVP 2.0 can be used for other locations with tailored RFP and SF values. For region/country with massive dust movements, the soiling model can be tuned in a

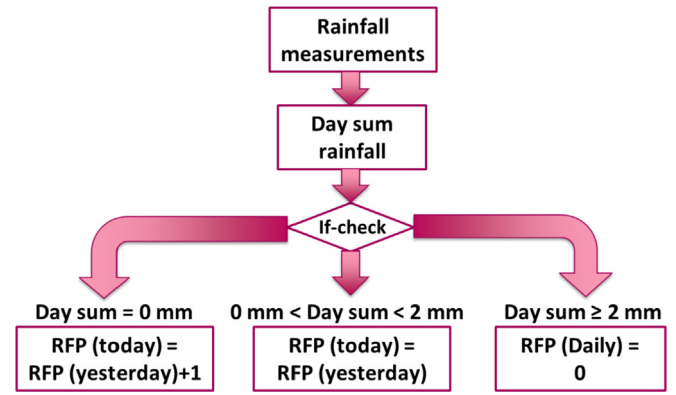


Fig. 3. Determination of the daily RFP in the PVP 2.0 model.

way that SF value changes automatically after detecting dust event trajectories [27]. It is worth noting that storm events contribute to both dust removal and dust deposition, therefore, they are not included in the RFP model.

3.2.3. Reflectance

The third light capture loss considered in the model is angular reflectance of sunlight from the panel surface. In contrast with the STC performance, sunlight falls on the panel in non-normal angles and therefore the reflectance from the panel surface is larger than at STC [28]. It is estimated that for commercial modules about 4% of G_{PoA} is lost annually due to reflectance, which is the fixed reflectance loss applied in the PVP 2.0 model [29] ($\eta_{reflectance} = 96\%$).

3.3. PV system conversion efficiency

Two main factors cause the PV system efficiency to be lower than the expected STC efficiency. Firstly, non-STC temperature and irradiance lead to different module efficiency, and secondly, BoS PV system components cause losses in the transport and conversion of electricity produced by the modules. Starting from STC efficiency, the PVP 2.0 applies a *chain of efficiencies* model to calculate the system efficiency up to the AC side (i.e. the grid), mathematically stated as:

$$\eta_{PV} = \eta_M(T_M, G_{PoA}) \cdot \eta_{cable} \cdot \eta_{MM} \cdot \eta_{MPPT} \cdot \eta_{inv} \quad (5)$$

where the factor $\eta_M(T_M, G_{PoA})$ represents the temperature- and irradiance-corrected module efficiency. The efficiencies after the module efficiency correspond, respectively, to the effects of Ohmic cabling losses, module mismatch, maximum power point tracking, and conversion from DC to AC electricity by the inverter.

STC module efficiency can be retrieved from the manufacturer datasheets. The calculations of the subsequent efficiencies in the chain are described in the following subchapters.

3.3.1. Irradiance

The effect of irradiance intensity on module efficiency is not usually communicated by commercial module manufacturers [30]. To estimate the effect of irradiance, the PVP 2.0 adopted a logarithmic relation between irradiance and efficiency, based on the behavior of external parameters in a single diode model [29]. According to this model, short-circuit current (I_{SC} , in Ampère) corresponds linearly to irradiance intensity:

$$I_{SC}(G_{PoA}) = I_{SC}(G_{STC}) \cdot \frac{G_{PoA}}{G_{STC}} \quad (6)$$

Fill factor (FF) is assumed to be independent of irradiance. Open-

circuit voltage (V_{OC} , in Volt) is dependent on irradiance according to the following relation:

$$V_{OC}(cell, G_{PoA}) = V_{OC}(cell, G_{STC}) + \frac{n \cdot k_B \cdot T}{q} \ln \frac{G_{PoA}}{G_{STC}}, \quad (7)$$

where $V_{OC}(cell, G_{PoA})$ is the V_{OC} (in Volt) of a single solar cell under the real PoA irradiance, $V_{OC}(cell, G_{STC})$ is the V_{OC} (in Volt) at STC as taken from the module datasheet, n is the diode ideality factor (which normally lies between 1 and 2), k_B is the Boltzmann constant ($1.38 \text{ E}^{-23} \text{ J/K}$), T is the module temperature (assumed equal to the STC temperature of 298.15 K), and q is the elementary charge ($1.602 \text{ E}^{-19} \text{ C}$). The equation is valid for a single cell. To find the V_{OC} of the entire module, the formula needs to be multiplied by the number of cells connected in series in the module. The model neglects the occurrence of a voltage drop due to the series connection.

With the I_{SC} , V_{OC} , and FF, the irradiance-dependent efficiency of the module $\eta_M(T_{STC}, G_{PoA})$ can be calculated by multiplying the three factors and dividing them by the incident irradiance G_{PoA} and the module surface area A_{PV} :

$$\eta_M(T_{STC}, G_{PoA}) = \frac{I_{SC} \cdot V_{OC} \cdot FF}{G_{PoA} \cdot A_{PV}} \quad (8)$$

3.3.2. Temperature

The effect of module temperature on efficiency can be evaluated independently from the irradiance effect. Commonly, module manufacturers list the (inverse linear) relation between module temperature and efficiency or power in the datasheet, as a temperature coefficient $d\eta/dT$ or dP/dT (in %/K). To determine the temperature-dependent module efficiency $\eta_M(T_M, G_{STC})$, the module temperature coefficient is necessary as well as the deviation of module temperature from STC temperature:

$$\eta_M(T_M, G_{STC}) = \eta_M(T_{STC}, G_{STC}) - \left(\frac{d\eta}{dT} \cdot (T_M - T_{STC}) \right) \quad (9)$$

In the PVP 2.0, module temperature is calculated by applying the Fuentes fluid-dynamic (FD) model. This model calculates the steady-state temperature of a flat plate via a heat balance between the plate and its environment [31]. The FD model requires the input of the weather data stored in the PVP 2.0 database, combined with module characteristics.

3.3.3. Module efficiency

The effect of irradiance and the effect of temperature on module efficiency have been evaluated separately in section 3.3.1 and 3.3.2. By applying the superposition principle, the combined effect of irradiance and temperature can be calculated as:

$$\eta_M(T_M, G_{PoA}) = \frac{\eta_M(T_{STC}, G_{PoA}) \cdot \eta_M(T_M, G_{STC})}{\eta_M(T_{STC}, G_{STC})} \quad (10)$$

3.3.4. Additional DC component losses

In a grid-connected PV system, commonly multiple modules are connected and the electricity from the module strings is transmitted to an inverter where DC-AC conversion takes place. At the DC side, the PVP 2.0 model assumes several small fixed efficiency losses.

Module mismatch losses occur when modules in a string produce different currents which lead to power dissipation in the string. Ohmic cabling losses are due to the electrical resistance of

the cable. Module mismatch losses are estimated at 1.5% and Ohmic cabling losses at 0.5% [29].

A third DC component loss is assigned to maximum power point tracking (MPPT). MPPT refers to a software algorithm that can calculate the optimal operating voltage of a PV module. A physical DC-DC converter then sets this operating voltage for the PV module [32]. Therefore, two efficiencies can be distinguished: the effectiveness of the algorithm in pinpointing the real MPP (the software efficiency), and the energy loss in the DC-DC converter (the hardware efficiency) [32].

A DC-DC converter for MPPT is commonly incorporated in grid-connected inverters [33]. The hardware efficiency of the MPPT is therefore included in the inverter efficiency model discussed in the next subsection. The software efficiency is commonly assessed via experiments under constant and under variable irradiance conditions, yielding a static and dynamic efficiency, respectively [33]. Averaging the static and dynamic efficiency yields the MPPT software efficiency, equivalent to the η_{MPPT} in this paper. In the PVP 2.0, a value for η_{MPPT} was taken based on the research of [34]. The static and dynamic efficiency of the two most common MPPT algorithms, Perturb and Observe (P&O) and Incremental Conductance (IC), were simulated, and yielded an average η_{MPPT} of 96.85% [34]. This is the value applied in the PVP 2.0 as well.

3.3.5. Inverter efficiency

The PVP 2.0 applies a dynamic inverter efficiency model developed by Sandia National Laboratories (SNL) [35]. The inverter efficiency in the SNL model includes the DC-DC converter efficiency of the MPPT block.

In the SNL model which is based on experimental measurements, inverter efficiency drops significantly as input power approaches zero. The realization that inverter efficiency is low at inputs far below the rated inverter power provides a cue for the selection of the appropriate inverter size for a PV system within the SNL database of characterized commercially-available inverters. Research of Hernández Castro Barreto et al. applied this insight to develop an *inverter sizing factor* (ISF) which determines the optimal inverter size based on the orientation of the PV modules [36]. The orientation-dependent ISF has been integrated into the PVP 2.0 as an improvement on fixed inverter size selection methods.

The further the tilt and azimuth of a PV system deviate from the optimal module orientation, the less frequent the number of hours will be in which the PV systems achieve a high-power output. In the Netherlands, PV systems achieve their rated power output only during a small fraction of the year. Thus, it will be beneficial to choose a smaller inverter to boost the DC-AC conversion efficiency. For each combination of tilt and azimuth, an ISF has been calculated for the Netherlands by Ref. [9]. By dividing the rated system power by the ISF, the optimal rated inverter power can be calculated.

Fig. 4 shows the benefit an undersized inverter can have compared to an inverter that matches the rated system capacity. A north-facing 1635 W_p PV system with a 40° tilt is used, which leads to an ISF of 204%. Due to the non-optimal orientation, PV production in all hours will be far below the installed capacity. A small inverter, therefore, more closely matches the power produced by the system, resulting in a larger DC-AC efficiency and reduced installation costs.

4. System efficiency breakdown

The PVP 2.0 website summarizes the power losses in an innovative interactive chart displaying the system efficiency over the current day.

Next to the losses described in Section 3, the chart also incorporates the material-dependent losses contributing to the

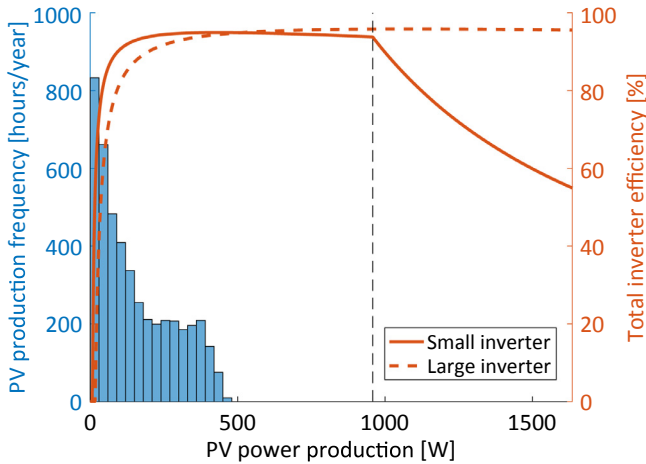


Fig. 4. PV system power output and the respective efficiencies of a small inverter selected with the ISF and a large inverter with an input capacity equal to the installed PV capacity of 1635 W_p . The grey vertical line denotes the small inverter capacity. If this capacity is exceeded, the inverter dissipates all excess power.

theoretical efficiency limit, i.e. thermalization, non-absorption, and bandgap utilization [37]. In addition, a fourth photovoltaic conversion loss called ‘opto-electrical loss’ is calculated as the difference between the theoretical efficiency limit and the STC efficiency of the specific module [38].

Fig. 5 is a screenshot of an efficiency breakdown chart on the PVP 2.0 website. The purpose of this figure is to provide users insight into the dominant loss factors in a PV system and into the steps through which the final system efficiency is arrived at in the PVP 2.0.

5. Dutch national solar electricity production

By using the meteorological data (described in section 2) as input into the performance model (described in section 3), the PVP 2.0 is able to calculate the real-time and annual performance of a designed PV system. This is put into practice by modeling and showcasing the real-time performance of a 6.9 MW_p simulated PV system case study on the website. The case study page reports the system’s annual energy production since its inception in 2014, as well as the amount of CO_2 emissions from conventional electricity generation sources that could have been avoided if the case study

PV system were to be installed.

The PVP 2.0 model can also be used to simulate the performance of a large number of PV systems to yield a cumulative performance estimate. It can, therefore, be applied to calculate an estimate of the cumulative power production of all PV systems in the Netherlands. Such an estimate is valuable for common citizens as well as policymakers, as it makes the impact of solar electricity on the national level tangible.

The flowchart of the model to calculate cumulative Dutch solar power production is represented in Figure A-4 in Appendix A. To establish an estimate, it is first necessary to create a set of PV systems that is representative of the characteristics of the entire installed capacity in the Netherlands. Statistical data on each of the six system characteristics (installation region, PV module technology, tilt, azimuth, PV system type (field or BAPV), and rated kW_p) required as input in the PVP 2.0 model were collected from governmental, commercial, and scientific reports and datasets. Besides, an estimate of the solar electricity capacity (in MW_p installed) was made to determine the potential national production. The most important public sources consulted are the *Nationale Solar Trendrapport*, data of the Dutch Central Bureau of Statistics (CBS), and the *Klimaatmonitor* [39–41]. Additional confidential datasets were provided by Solar Monkey, Eindhoven University of Technology (TU/e), and the Dutch transmission service operators (TSOs) Stedin and Alliander.

Each characteristic contains a set of options, each with its specific share (in %) of the total population. For example, the national installed capacity is spread over 12 provinces in the Netherlands, so each province will contain a certain share of the total installed PV capacity, as shown in Fig. 6.

By multiplying the number of options of each characteristic, a total set of 475 PV system designs, each with unique characteristics was created: a *system design portfolio*. To show how this portfolio calculation works, imagine that only two characteristics are relevant: the module tilt and azimuth. Imagine also that in the Netherlands, two options exist for system tilt: 40% of systems have a 15° tilt, and 60% a 40° tilt. Similarly, three options exist for azimuth: southeast (20%), south (60%) and southwest (20%). This would result in six unique system designs in the portfolio, each with a respective share: a system with 15° tilt and southeast azimuth would represent 8% of all systems, while a 40° tilt and south-facing system would be more common, representing 36% of the total installed capacity.

With the characteristics defined for each of the systems in the

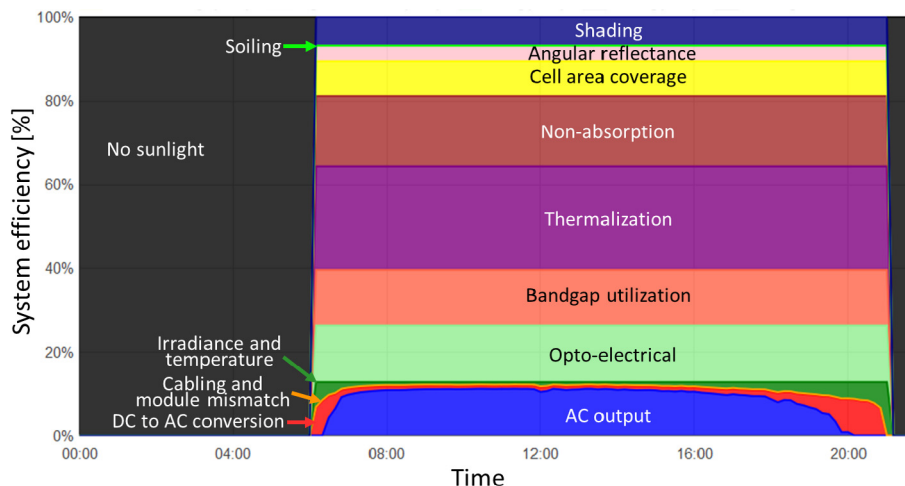


Fig. 5. Efficiency breakdown for a CIGS-based PV system. The bottom blue area displays the final system efficiency. When the Sun is below the horizon, system efficiency goes to zero and the figure displays only one value for “No sunlight”.

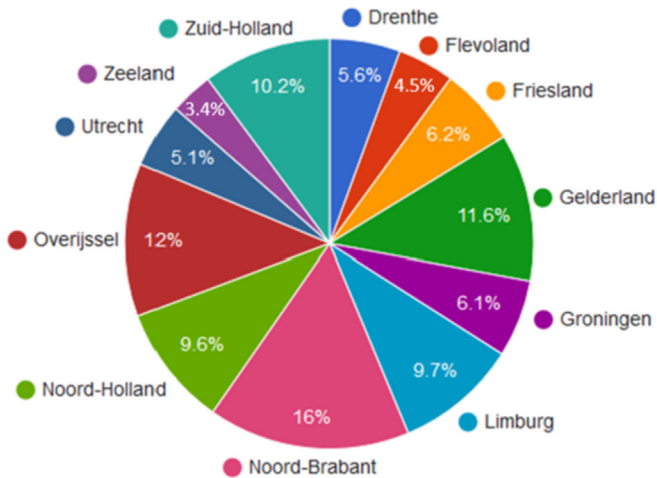


Fig. 6. Distribution of installed solar capacity over the twelve Dutch provinces. Data are taken from Ref. [41].

portfolio, the real-time performance for each system is calculated. Using the relative share of each system in the portfolio, a weighted average performance is calculated for the portfolio, expressed as the instantaneous electricity yield (IEY) in W/W_p (i.e. which percentage of the rated installed power is achieved at that moment). The portfolio IEY is calculated for each of the 12 Dutch provinces. By multiplying the IEY by the total installed capacity in each province, the total power production in each province is found. By adding up the power production of every province, the national solar electricity production (NSEP) is calculated.

Fig. 7 shows the NSEP as calculated by the PVP 2.0. It can be seen that changes in the meteorological conditions and Sun position affect the NSEP during the day.

The PVP 2.0 database has stored all power production values of each province and the national total solar power production since 31 January 2018, with a 10-min time resolution.

Validation of the accuracy of the NSEP model is planned in the future development of the PVP 2.0. One weakness of the PVP 2.0 NSEP model is that it requires specific and representative information on PV system characteristics and installed capacity that is

sometimes absent or outdated. The NSEP model, therefore, requires active maintenance and data collection to ensure an up-to-date and improved estimate of national production. While the results found in this section are specific to the Netherlands, the approach used can be applied to any country of interest provided there are sufficient data on the installed capacity and its characteristics in the country.

6. Economic analysis

The fifth and final element implemented in the PVP 2.0 was the economic analysis. The motivation for its inclusion is that monetary considerations are an important factor in the decision of households or companies to invest in a PV system [42].

For creating the profitability analysis, based on scientific literature research [43–45] and an evaluation of PV websites [4,7], four economic indicators were taken into account. A flowchart of the complete profitability analysis in the PVP 2.0 is shown in Figure A-5 of Appendix A.

The first indicator is the net present value (NPV, in €) of the PV system. The NPV is the current value of the profit (or loss) made over the investment lifetime [43].

The second indicator, the payback period (PBP, in years) indicates the amount of time it will take for the total profit to outweigh the initial investment [43].

The compound annual growth rate (CAGR, in %) indicates the average annual interest made over the total investment [45]. The CAGR of the PV system can be compared with the standard interest rate expected by website users.

The fourth and final indicator is levelized cost of electricity (LCoE, in €/kWh). The LCoE represents the amount of money it costs to produce one kWh of electricity [44]. The LCoE is an indicator through which the cost-competitiveness of PV versus other energy generation technologies can be compared [44].

Six parameters are required for the calculations of the four indicators: (1) PV system lifetime, (2) the initial investment cost, (3) the annual operation and maintenance (O&M) cost, (4) the annual energy production (which includes a panel degradation factor leading to decreased production over time), (5) the annual revenue, and (6) the discount rate [43–45]. Values for each of these parameters applicable for the Netherlands were found through literature research and commercial information supplied by PV system

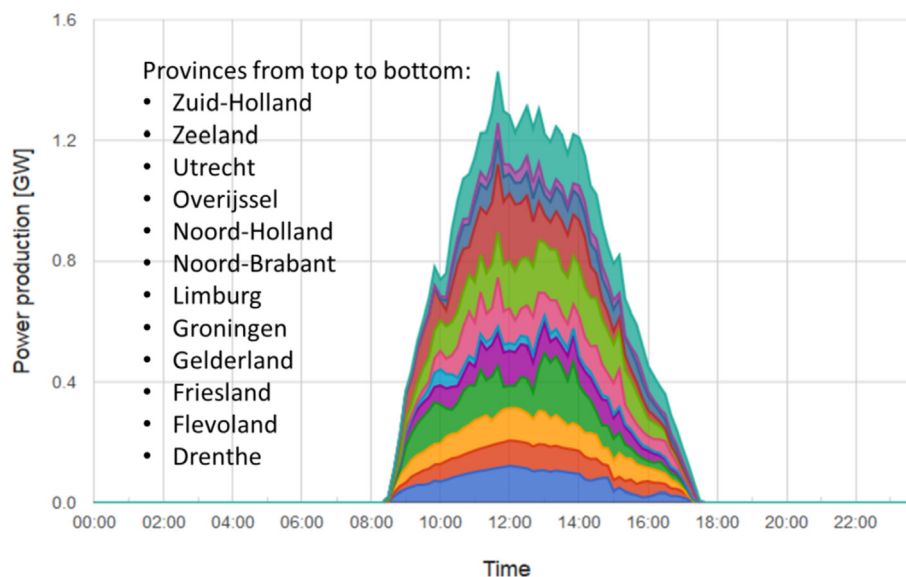


Fig. 7. Screenshot of the Dutch NSEP composed of the provincial productions for 6 February, 2018.

retailers [39,42,44,46–52]. Government subsidies and tax breaks are included in the PVP 2.0 analysis.

There is no universally accepted method in determining the appropriate discount rate, but its value can have a decisive impact on the attractiveness of an investment [44]. Therefore the PVP 2.0 includes three discount rate scenarios (similar to the approach used by Ref. [44]): one in which it is neglected (0%), a medium rate (3%), and a high discount rate (7%). The benefit of this multi-scenario approach is that it provides insight in how decisive the discount rate can be on perceived system profitability.

Whenever a user designs a system in the PVP 2.0, the system design choices are used to calculate the total system costs whereas the annual energy production is used to calculate the total annual revenue. A screenshot of the calculation outcome for a 1 kW_p south-facing BAPV system with mono-Si modules is shown in Fig. 8.

Whereas the real profit increases steadily from year to year, the net present value is lower due to the discounting of future profits. PV systems with higher initial investment and/or a lower annual energy production can have negative NPVs, even if the total profit after 25 years is positive. This simply indicates that the investment would be less attractive than one with an interest rate equal to the discount rate.

Profitability of the system is sensitive to the PV module choice, the orientation, and the choice of system type. The monetary gains of selling the additional electricity produced by a higher-efficiency module do not outweigh the initial purchasing cost of this module. The further the module tilt and azimuth are away from the optimum orientation, the higher the LCoE and the lower the profitability due to the decreased energy generation. Finally, residential systems were found to be much more profitable than commercial systems because of the twice as high electricity price for consumers. This electricity revenue is enough to offset the larger initial investment for residential PV compared to commercial PV.

A profitability analysis by Ref. [53] found a payback period of 10 years for a 3.4 kW_p residential PV system in the Netherlands. The PVP 2.0 model found a similar payback period of 10 years for a PV system with the characteristics used in the calculations of [53], supporting the validity of the PVP 2.0 analysis.

In the Netherlands, the profitability of PV depends to a large extent on the generous net metering policy for residential PV systems and the renewable energy subsidy for commercial PV systems [53]. Potential changes in these government policies need to be monitored to ensure the continued reliability of the economic model.

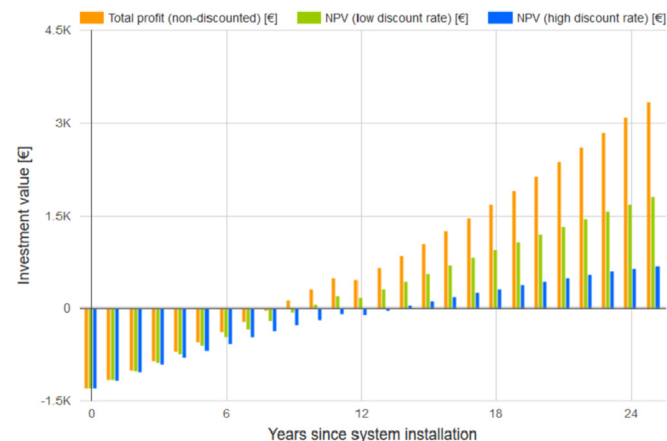


Fig. 8. Screenshot of the economic analysis chart on the website. The evaluated system is a 1 kW_p south-facing BAPV system with mono-Si modules.

7. Yield comparison and sensitivity study

7.1. Yield comparison

As a first validation of the PVP 2.0 performance model, a dataset of installed (rooftop) PV systems provided by Solar Monkey was used to compare measured AC energy values (kWh/year) with AC energy values calculated with the PVP 2.0. The dataset contains 26 carefully-selected systems, varying in configuration, location, size and module technology. The performance model was run with user input corresponding the best possible to the characteristics of the Solar Monkey systems.

It was found that deviations from the measured AC energy values range from roughly -15% to $+15\%$. These calculations use the fixed shading factor as mentioned in 3.2.1. When eliminating this effect by using a calculated shading factor for each system based on a horizon profile, the error range drops to -11% to $+5.5\%$. Fig. 9 shows the deviation for each system. These deviations could be caused by the fact that the inverter model cannot properly deal with systems containing multiple azimuth configurations or multiple inverters. In 84.6% of the cases (22 out of 26), the deviation is negative, which implies that the performance model underestimates the AC energy yield. One reason for this could be a possible overestimation of shading loss due to imprecise shading factors.

7.2. Sensitivity study

To investigate the effect of non-STC temperature and irradiance on PV modules due to meteorological conditions, a sensitivity study was conducted. While certain studies are common on module level, the PVP 2.0 provides the possibility to perform such an analysis on a province or even national level, by using a system design portfolio as described in section 5. At this point, the PVP 2.0 user cannot perform such analysis themselves since this requires back-end manipulation of the weather parameters. However, the results of this study potentially could provide quantitative insights on the impact of changing the climate on solar energy production within a country.

This study consists of three cases: (1) change in ambient temperature on average during a year, (2) change in average wind speed during a year, and (3) a rain-free Summer. A comparison was made between the AC energy yield values of a ‘normal average year’ (using the untouched climate database) and the AC energy yield values calculated with adjustments related to the specific case.

For cases (1) and (2), annual calculations were done for the province ‘Zuid-Holland with a capacity of 411 MW_p (estimation based on [39–41]) and a variety of systems. In case (3), a Summer period is considered for just one system (100 PV modules) located in the city of Rotterdam. By using just one system in this case, calculation-time is reduced. Due to the characteristics of the soiling model, the calculated

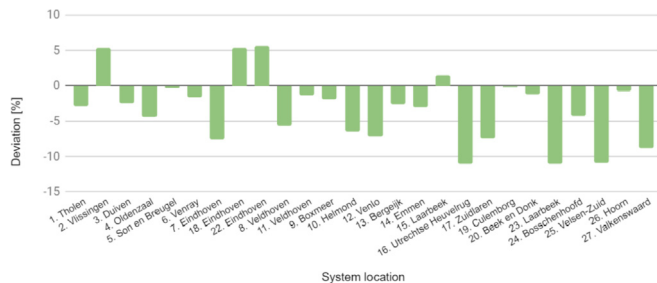


Fig. 9. Calculated annual AC energy deviation with respect to the measured annual AC energy values of each Solar Monkey system. In 84.6% of the cases the deviation is negative leading to average deviation of -3.25% , which shows an underestimation by the PVP 2.0 model.

Table 2
Results of the sensitivity study cases (1), (2) and (3).

Case number (1.A-D), (2.A-C): yearly calculations for 'Zuid Holland' (3): 92 days in summer for the system in Rotterdam	AC energy change [GWh/year]	AC energy change [%/year]	AC Yield [kWh/kWp]
(1.A) Ambient Temperature +10%	-2.19	-0.58	918.43
(1.B) Ambient Temperature -10%	+2.19	+0.58	929.11
(1.C) Ambient Temperature +3 °C	-4.40	-1.16	913.13
(1.D) Ambient Temperature -3 °C	+4.38	+1.16	934.51
(2.A) Wind speed +10%	+0.93	+0.24	926.10
(2.B) Wind speed -10%	-1.02	-0.27	921.35
(2.C) Wind speed, doubled	+6.42	+1.69	939.49
(3) Rain-free summer (92 days)	-297.5 [kWh/Summer]	-3.4 [%/Summer]	

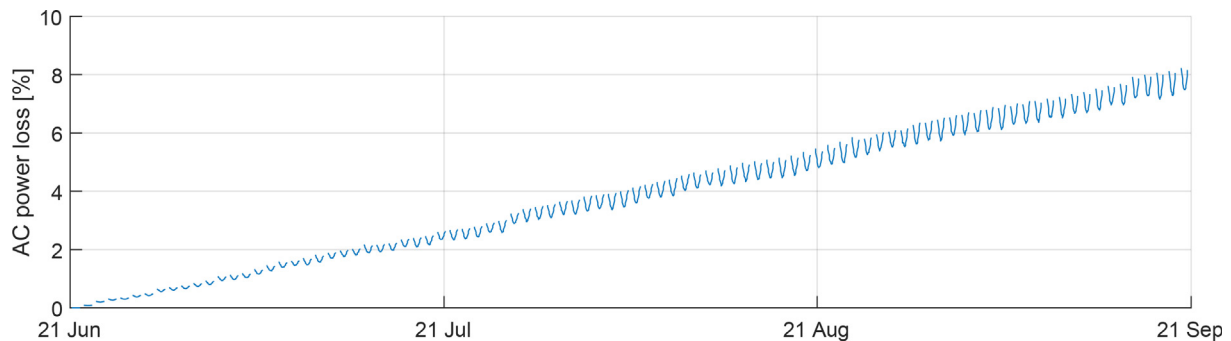


Fig. 10. AC power loss per day in a summer with no rain in comparison to a normal average summer (for a system with 100 modules located in Rotterdam, 27 kW_p).

results are valid on the province level as well. The percentage of changes in AC energy values are presented in Table 2.

A 10% change in ambient temperature causes an energy gain/loss of 0.58%/year, while a 3 °C shift even has a stronger effect of 1.16%/year, which corresponds to 4.4 GWh/year. Within the range of 10% change, wind speed is found to less strongly affect the AC energy with around 0.25%/year. However, due to the logarithmic wind-profile law used in the FD model [54], this effect can become stronger when larger ranges are considered (for example in case 2.C, where the wind speed is doubled and this results in a gain of 1.69%/year).

In case (3), the accumulating soiling loss due to a constantly increasing RFP results in a 3.4% AC energy loss during 92 days. In Fig. 10, it can be seen that this results from the daily increasing power loss (%). The 'v-shaped' curves show that the percentage power loss is higher during times with low irradiance (morning and evenings) and there is an average power loss of approximately 3.5%.

While these calculations are the first estimate, they illustrate that the effect of soiling can be quite significant in a period without rain (or cleaning) and that on large scale, the impact of a small change in climate conditions could lead to losses around 2–4.5 GWh/year.

8. Conclusions

This paper has aimed to communicate in detail the framework through which the PVP 2.0 modeling environment was developed, thereby allowing other researchers to apply (parts of) the methodology to any country of interest. The development of the website has shown the importance of having access to reliable short-term and long-term meteorological data. In the development of the PVP 2.0, several innovative concepts not present in other PV system modeling websites have been implemented: a dynamically updated climate database, rainfall-dependent soiling losses, orientation-dependent inverter size selection, and an interactive chart of PV system efficiency. The model consists of a set of independent calculation blocks, each block can be improved by incorporating new scientific insights without affecting the accuracy of other calculation steps in the performance model.

The creation of a meteorological database and PV system performance model are at the core of any PV modeling environment. This core is multifaceted and can be utilized to model several other topics related to PV. In the PVP 2.0, the core was used to create (1) an overview figure of all real-time efficiency losses in PV systems, (2) an estimate of the Dutch national solar electricity production, (3) an economic analysis of user-designed PV systems, and (4) a tool for sensitivity study of solar energy production to climate/weather variation scenarios.

The yield comparison study was done as the first validation of the performance of PVP 2.0. With the sensitivity study, a first step is made in providing quantitative insights into the impact of changing the climate on solar energy production within a country. Results of such a study are estimates, but illustrate the potential of the performance model for large scale impact calculations. In future website development, the current range of functionalities will be expanded, encompassing a wider range of mounting solutions (e.g. East-West configuration or ground cover ratio as input), modeling of storage and improved graphic user interface.

Declaration of competing interest

None.

Acknowledgments

The authors would like to thank the Koninklijk Nederlands Meteorologisch Instituut (KNMI) for providing real-time meteorological data and the companies of Solar Monkey BV and Stedin for providing valuable PV system datasets for this research. Pramod Nepal and Sandeep Mishra are gratefully acknowledged for useful discussions.

APPENDIX

Appendix A. Flowcharts summarizing the components of the PVP 2.0.

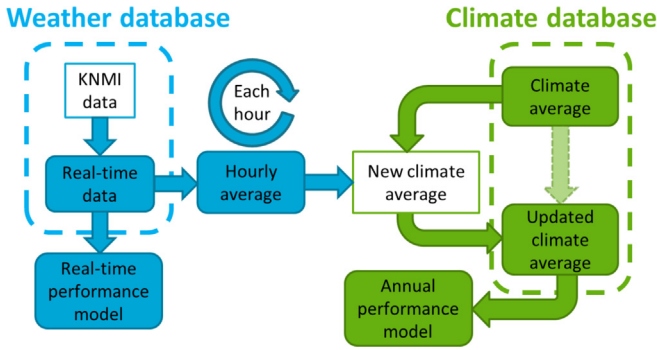


Fig. A-1. Connection between the real-time and climate database. The creation of a weighted average of the new and historical measurements allows the annual dataset to become dynamic.

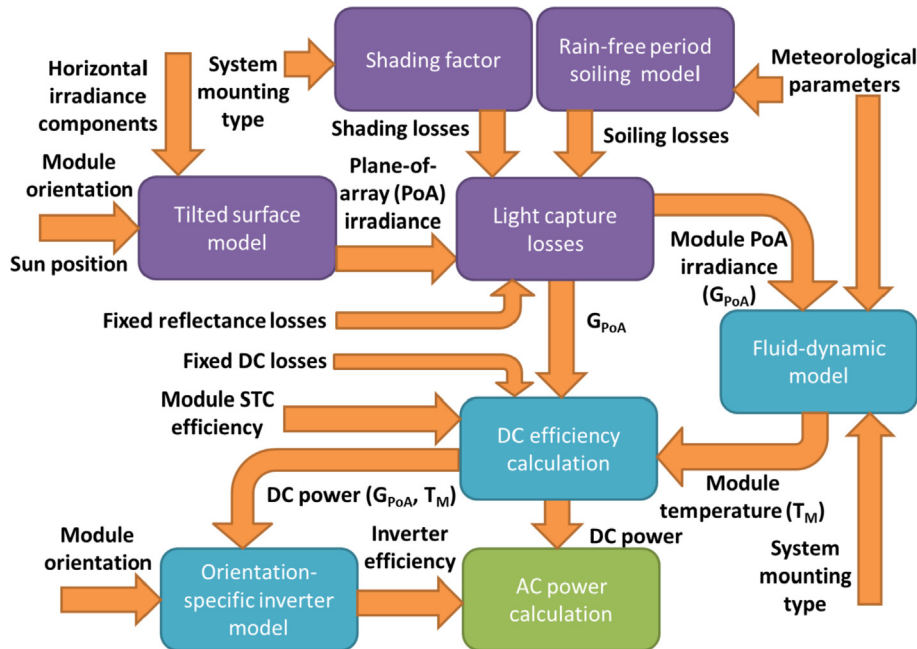


Fig. A-2. Overview of the PVP 2.0 PV system performance model. The purple boxes indicate factors related to light capture, the blue boxes are related to internal PV system factors, and the green box is the objective of the performance calculation.

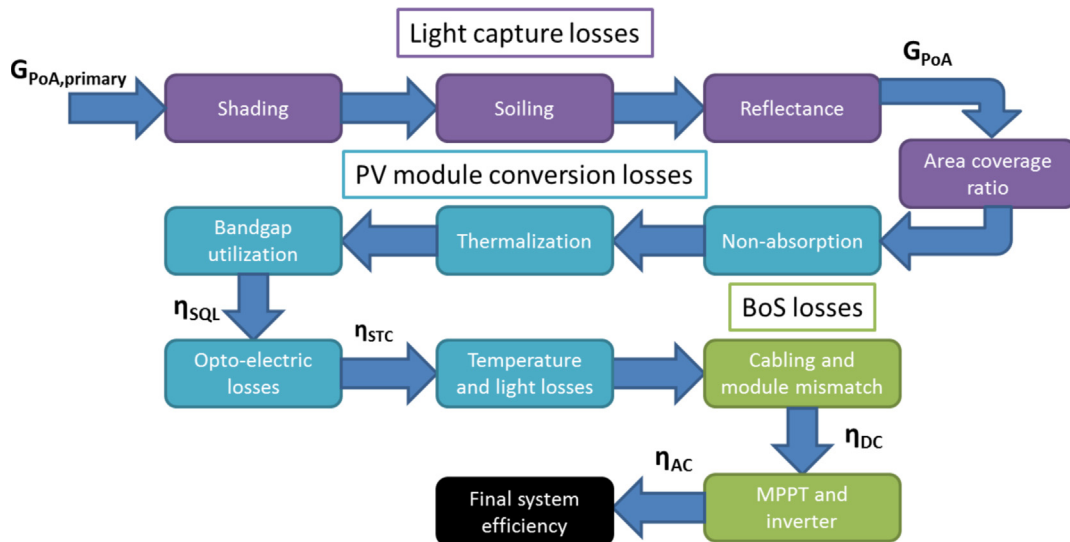


Fig. A-3. Efficiency losses considered in the system efficiency breakdown. The different box colors categorize the losses.

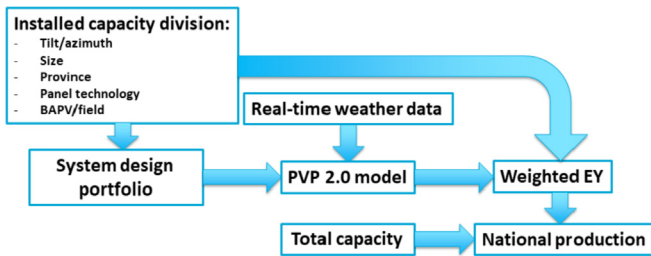


Fig. A-4. PVP 2.0 NSEP real-time estimation model. EY refers to electricity yield in W_p .

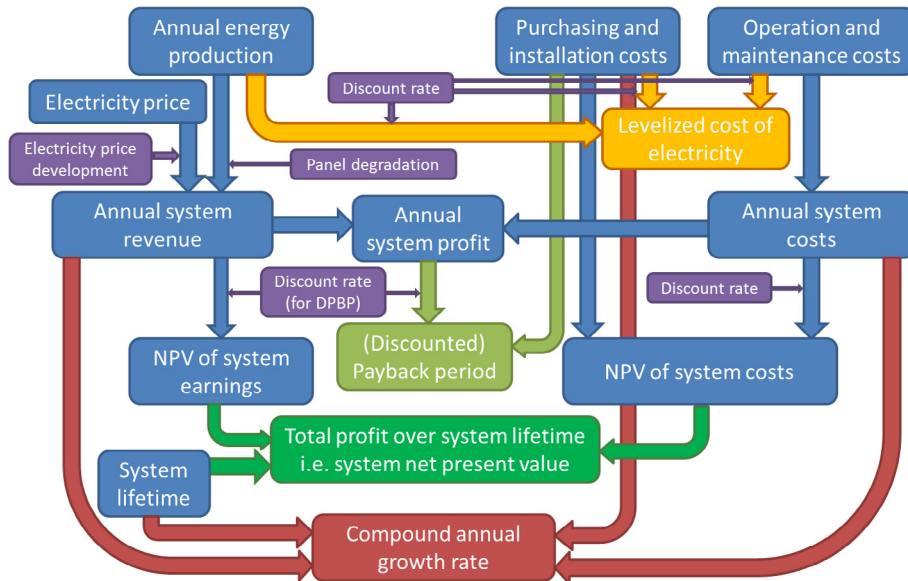


Fig. A-5. Overview of the general model to calculate four economic analysis indicators. Blue boxes are numerical inputs and purple boxes are factors influencing these numerical inputs over the system lifetime.

References

[1] SolarPower Europe, Global market outlook for solar power 2019 - 2023, in: SolarPower Europe, Tech. Rep., 2019, Belgium.

[2] S. Honsberg, Christiana, Bowden, PV education [Online]. Available: pveducation.org/, 2018. (Accessed 5 June 2018).

[3] Sandia National Laboratories, PV Performance Modeling Collaborative, 2018 [Online]. Available: pvpmc.sandia.gov/. (Accessed 5 June 2018).

[4] SMA Solar Technology, "Sunny Design Web, 2018 [Online]. Available: <https://www.sunnydesignweb.com/sdweb/#/Home>. (Accessed 5 June 2018).

[5] European Commission, Photovoltaic Geographical Information System, 2018 [Online]. Available: <http://re.jrc.ec.europa.eu/pvgis.html>. (Accessed 5 June 2018).

[6] Zonatlas, Zonatlas [Online]. Available: <https://www.zonatlas.nl/start/>, 2018. (Accessed 26 August 2018).

[7] Google, Project Sunroof, 2018 [Online]. Available: <https://www.google.com/get/sunroof#p=0>. (Accessed 5 May 2018).

[8] University of Ljubljana, PV portal slovenski portal za fotovoltaiiko [Online]. Available: <http://pv.fe.uni-lj.si/SEvSLO.aspx>, 2007. (Accessed 17 August 2018).

[9] O. Isabella, G. Ganesan Nair, A. Tozzi, J. Hernandez Castro Barreto, G.R. Chandra Mouli, F. Lantsheer, S. van Berkel, M. Zeman, Comprehensive Modelling and Sizing of PV Systems from Location to Load, vol 1771, 2015.

[10] PVsyst, PVsyst [Online]. Available: <http://www.pvsyst.com/en/>, 2012. (Accessed 26 August 2018).

[11] Meteonorm, Meteonorm [Online]. Available: <https://www.meteonorm.com/>, 2018. (Accessed 26 August 2018).

[12] Sungevity, Sungevity [Online]. Available: <https://www.sungevity.nl/>, 2018. (Accessed 26 August 2018).

[13] Solar Monkey, Solar Monkey [Online]. Available: <https://www.solarmonkey.nl/>, 2017. (Accessed 17 August 2018).

[14] D.T. Reindl, W.A. Beckman, J.A. Duffie, Diffuse fraction correlations, Sol. Energy 45 (1) (1990) 1–7.

[15] A. Smets, K. Jäger, O. Isabella, R. Van Swaaij, M. Zeman, Solar Energy: the Physics and Engineering of Photovoltaic Conversion, Technologies and Systems, first ed., UIT, Cambridge, United Kingdom, 2016.

[16] S. Pelland, C. Maalouf, R. Kenny, L. Leahy, B. Schneider, G. Bender, Solar energy assessments: when is a typical meteorological year good enough?, in: SOLAR 2016 - American Solar Energy Society National Solar Conference 2016 Proceedings, 2016, pp. 77–83.

[17] National Renewable Energy Laboratory, Weather data [Online]. Available: <https://sam.nrel.gov/weather>, 2014. (Accessed 1 March 2018).

[18] World Meteorological Organization, FAQs - climate [Online]. Available: <https://public.wmo.int/en/about-us/FAQs/faqs-climate>, 2016. (Accessed 10 May 2017).

[19] Meteonorm, Handbook Part II: Theory, Bern, Switzerland, 2017.

[20] D. Palmer, I. Cole, T. Betts, R. Gottschalg, Interpolating and estimating horizontal diffuse solar irradiation to provide UK-wide coverage: selection of the best performing models, Energies 10 (2017) 2.

[21] D.T. Reindl, W.A. Beckman, J.A. Duffie, Evaluation of hourly tilted surface radiation models, Sol. Energy 45 (1) (1990) 9–17.

[22] M. Santamouris, Appropriate materials for the urban environment, in: M. Santamouris (Ed.), Energy and Climate in the Urban Built Environment, Routledge, Abingdon, United Kingdom, 2011, pp. 160–180.

[23] R. Levinson, H. Akbari, M. Pomerantz, S. Gupta, Solar access of residential rooftops in four California cities, Sol. Energy 83 (12) (2009) 2120–2135.

[24] P. Nepal, et al., Accurate soiling ratio determination with incident angle modifier for PV modules, IEEE J. Photovolt. 9 (1) (2018) 295–301.

[25] P. Nepal, Effect of Soiling on the PV Panel kWh Output, Delft University of Technology, 2018.

[26] A. Kimber, L. Mitchell, S. Nogradi, H. Wenger, "The effect of soiling on large grid-connected photovoltaic systems in California and the southwest region of the United States, in: 2006 IEEE 4th World Conference on Photovoltaic Energy Conference vol 2, 2006, pp. 2391–2395.

[27] J. Bilbao, et al., UV and global irradiance measurements and analysis during the Marsaxlokk (Malta) campaign, Adv. Sci. Res. 12 (1) (2015) 147–155.

[28] A.M. Gracia, T. Huld, Performance Comparison of Different Models for the Estimation of Global Irradiance on Inclined Surfaces, Publications Office of the European Union, Luxembourg, 2013.

[29] A. Smets, K. Jäger, O. Isabella, R. Van Swaaij, M. Zeman, PV system design, in:

- Solar Energy: the Physics and Engineering of Photovoltaic Conversion, Technologies and Systems, first ed., UIT, Cambridge, United Kingdom, 2016, pp. 317–350.
- [30] H. Ziar, B. Asaei, S. Farhangi, M. Korevaar, O. Isabella, M. Zeman, Quantification of shading tolerability for photovoltaic modules, *IEEE J. Photovolt.* 7 (5) (2017) 1390–1399.
- [31] M.K. Fuentes, A Simplified Thermal Model for Flat-Plate Photovoltaic Arrays, Sandia National Labs., Albuquerque, NM (USA), 1987.
- [32] M. Müller, R. Bründlinger, O. Arz, W. Miller, J. Schulz, G. Lauss, PV-off-grid hybrid systems and MPPT charge controllers, a state of the art analyses, *Energy Procedia* 57 (2014) 1421–1430.
- [33] M. Valentini, A. Raducu, D. Sera, R. Teodorescu, PV inverter test setup for European efficiency, static and dynamic MPPT efficiency evaluation, in: 2008 11th International Conference on Optimization of Electrical and Electronic Equipment, 2008, pp. 433–438.
- [34] B. Bendib, H. Belmili, F. Krim, A survey of the most used MPPT methods: conventional and advanced algorithms applied for photovoltaic systems, *Renew. Sustain. Energy Rev.* 45 (2015) 637–648.
- [35] W.E. Boyson, G.M. Galbraith, D.L. King, S. Gonzalez, Performance Model for Grid-Connected Photovoltaic Inverters, Sandia National Laboratories, Albuquerque, New Mexico, USA, 2007.
- [36] J. Hernández Castro Barreto, Optimizing Inverter Sizing for PV Systems According to Their Installation Characteristics, Delft University of Technology, 2014.
- [37] W. Shockley, H.J. Queisser, “Detailed balance limit of efficiency of p-n junction solar cells, *J. Appl. Phys.* 32 (3) (1961) 510–519.
- [38] A. Ingenito, O. Isabella, S. Solntsev, M. Zeman, Accurate opto-electrical modeling of multi-crystalline silicon wafer-based solar cells, *Sol. Energy Mater. Sol. Cells* 123 (2014) 17–29.
- [39] Solar Solutions Int, Nationaal Solar Trendrapport 2018, Haarlem, the Netherlands, 2018.
- [40] CBS, Hernieuwbare elektriciteit; productie en vermogen, 2016 [Online]. Available: <http://statline.cbs.nl/Statweb/publication/?DM=SLNL&PA=82610ned>. (Accessed 9 January 2017).
- [41] Rijkswaterstaat, Klimaatmonitor [Online]. Available: <https://klimaatmonitor.databank.nl/jive>, 2016. (Accessed 9 January 2017).
- [42] S. Rodrigues, R. Torabikalaki, F. Faria, N. Cafôfo, X. Chen, A.R. Ivaki, H. Mata-Lima, F. Morgado-Dias, Economic feasibility analysis of small scale PV systems in different countries, *Sol. Energy* 131 (2016) 81–95.
- [43] M. Bortolini, M. Gamberi, A. Graziani, C. Mora, A. Regattieri, Multi-parameter analysis for the technical and economic assessment of photovoltaic systems in the main European Union countries, *Energy Convers. Manag.* 74 (2013) 117–128.
- [44] IEA, Projected Costs of Generating Electricity - 2015 Edition, 2015. Paris, France.
- [45] Investopedia, Annual return [Online]. Available: <https://www.investopedia.com/terms/a/annual-return.asp>, 2018. (Accessed 17 February 2018).
- [46] C. Tjengdrawira, M. Richter, I. Theologitis, Best Practice Guidelines for PV Cost Calculation - Accounting for Technical Risks and Assumptions in PV LCOE, 2016. Bolzano, Italy.
- [47] T. Lang, E. Gloerfeld, B. Girod, “Don’t just follow the sun – a global assessment of economic performance for residential building photovoltaics, *Renew. Sustain. Energy Rev.* 42 (Feb. 2015) 932–951.
- [48] S. Philipps, W. Warmuth, Photovoltaics Report 2016, 2016. Freiburg, Germany.
- [49] IEA PVPS, Trends 2016, in: Photovoltaic Applications, 2016th ed, International Energy Agency, Paris, France, 2016.
- [50] D.C. Jordan, S.R. Kurtz, Photovoltaic degradation rates—an analytical review, *Prog. Photovolt. Res. Appl.* 21 (1) (Jan. 2013) 12–29.
- [51] CBS, Aardgas en elektriciteit, gemiddelde prijzen van eindverbruikers, 2017 [Online]. Available: <http://statline.cbs.nl/Statweb/publication/?DM=SLNL&PA=81309NED&D1=8&D2=0&D3=0&D4=19,24,29,34,39,44,49&HDR=T&STB=G2,G3,G1&CHARTTYPE=3&VW=T>. (Accessed 18 February 2018).
- [52] K. Schoots, M. Hekkenberg, P. Hammingh, Nationale Energieverkenning 2017, 2017. Petten, the Netherlands.
- [53] M.J. Kok, Voortzetten Salderingsregeling Absolute Voorwaarde Voor Zonnige Toekomst Particuliere Zonnestroominstallaties, K & R Consultants BV, 2016 [Online]. Available: <http://krcon.nl/voortzetten-salderingsregeling-absolute-voorwaarde-zonnige-toekomst-particuliere-zonnestroominstallaties>. (Accessed 6 June 2018).
- [54] S.A. Hsu, E.A. Meindl, D.B. Gilhousen, Determining the power-law wind-profile exponent under near-neutral stability conditions at sea”, *J. Appl. Meteorol.* 33 (6) (1994) 757–765.